Is There a Correlation Line for Hydrofoil Drag ?

Abstract. The ITTC-57 correlation line is still very popular for the prediction of the viscous resistance of hydrofoils. This paper answers the questions whether this is a valid assumption and in which cases it is possible to define a correlation line.

NOMENCLATURE

c	Chord length of foil	θ	Momentum thickness of b. l.
C_D	Total drag coefficient of foil	ν	Kinematic viscosity
C_F	Total skin friction coefficient of plate		
k	Height of roughness particle	Subscripts:	
l	Length of plate		
Re_c	Reynolds number $U_\infty \cdot c / \nu$	k	at the top of the particle
t	Maximum thickness of foil	*lam*	for laminar flow
u	Velocity within the boundary layer	*tr*	at location of transition
U	Velocity at the edge of the b. l.	*turb*	for turbulent flow
U_∞	Undisturbed velocity far in front of the foil	0	at location of trip
x	Distance from leading edge		

1. INTRODUCTION

Today's velocity prediction programs (VPP), e.g. [1], treat the keel and rudder as vertical hydrofoils. The physical model for the determination of the lift and drag forces of hydrofoils is taken from the theory of the airplane wing. Important input parameters to this model are the fluiddynamic characteristics of the profile sections. The most reliable source for the NACA wing sections is the compilation of experimental results by Abbott and Doenhoff [2]. A more modern approach is the computer program XFOIL [3] that determines the aerodynamic characteristics numerically. It employs a panel method for the solution of the potential flow and solves iteratively the integral boundary layer equations. The diagrams in [2] or the program XFOIL are convenient, when the geometry of the section as well as the speed and the angle of attack are fixed and known. In a VPP the difficulty arises that these quantities are not known up front, but are iteratively varying during the solution process. It is therefore desirable to have a closed form mathematical expression that can be used in the VPP for the computation of the lift and drag coefficients. To keep this paper to a moderate size its scope is limited to the determination of the drag coefficient at zero angle of attack. The chances for a general solution of the problem will be discussed at the end of the paper.

2. PREDICTION METHODS FOR THE DRAG COEFFICIENT

The theoretical determination of the drag of a wing section was initiated in 1937 by Squire and Young [4]. Based on Prandtl's boundary layer theory they calculated the two-dimensional profile drag as a function of the momentum thickness and the velocity at the trailing edge. These parameters depend on the geometry of the foil and on the chord based Reynolds number. In 1949 Helmbold [5] proved theoretically that the drag-function could be separated into a product of two functions, one of it being the friction coefficient for the turbulent flow over the flat plate. The second factor depends on the potential flow around the foil and on the transition point (equation 1)

$$C_D = C_{F,turb} \cdot f\left(\frac{U}{U_\infty}, \theta_{tr}, u_{tr}\right) \tag{1}$$

Hoerner [6] changed this function without proof and deleted the dependence on the transition point from the second factor. For a given profile family the second factor depends in this case only on the thickness ratio of the foil (equation 2). He proposed two different thickness functions, one for the NACA four-digit series and one for the NACA 6-series. The first factor is now not any more the friction coefficient for turbulent flow, but the coefficient for the mixed flow over the flat plate with the transition at the same location as on the foil.

$$C_D = C_F \cdot f\left(t/c\right) \tag{2}$$

Hoerner writes [6, p.6-5]: "The skin-friction drag also depends, of course, on the location of the boundary layer's transition point on section chord." Since the transition point is a function of the geometry of the foil, the angle of attack and the Reynolds number, we have nothing gained and are basically in the same situation as in the beginning. We could stop now and conclude that a correlation in functional form is not achievable. Nevertheless, many VPPs use correlation lines, so it would be interesting to analyze their validity. A second application of correlation lines is the analysis of towing tank experiments. Since the towing tank models usually employ a boundary layer trip to fix the transition at a given location, there is some hope that at least in these cases the drag forces will be predictable.

2.1 The thickness function in the drag coefficient

In the following analysis we will use the NACA 0012 profile section as a test case. For this profile family Hoerner proposes:

$$C_D = C_F \cdot \left[1 + 2 \cdot \frac{t}{c} + 60 \cdot \left(\frac{t}{c} \right)^4 \right] \tag{3}$$

In figure 1 Hoerner's curve is compared to the experimental results of Abbott and Doenhoff [2] for a fixed Reynolds number. As we are also interested in the drag coefficient with a boundary layer trip, a data point according to McCroskey [7] is added. McCroskey collected all available test results of the NACA 0012 wing section, grouped this large amount of data after their accuracy and calculated approximating curves for the best fit to the data. Because this paragraph only deals with the thickness function, the values of the coefficient C_F in equation 3 are chosen to make the dashed lines coincide with the 12% data points.

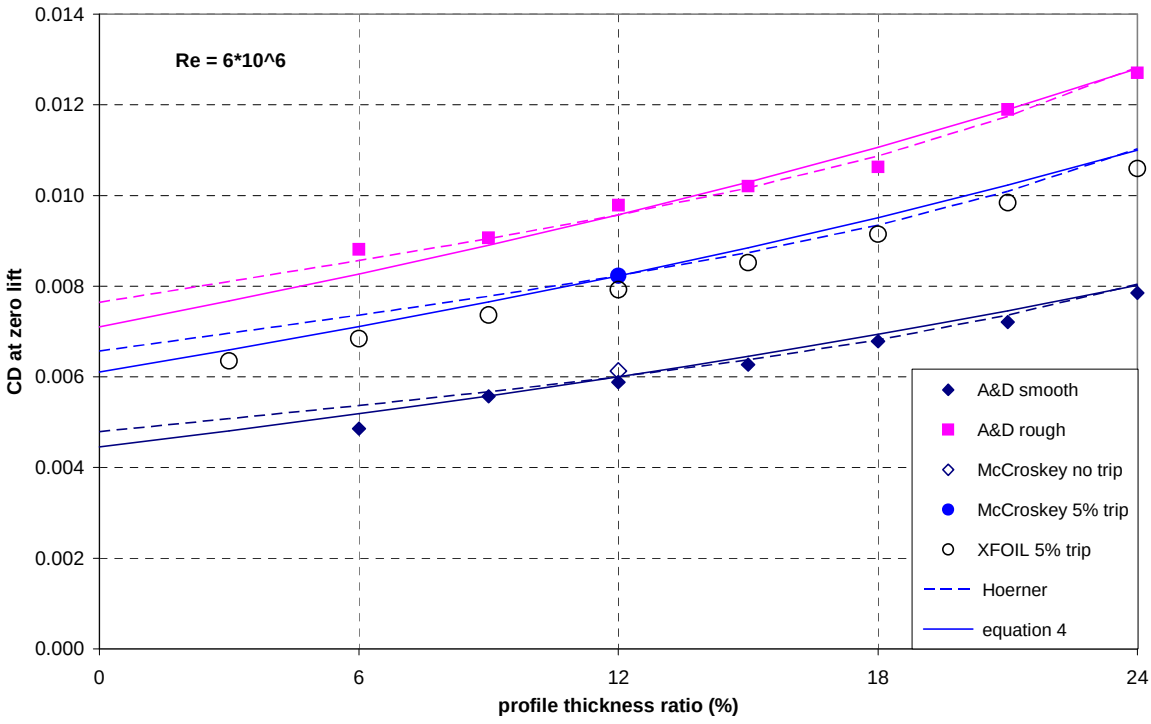

Figure 1. Thickness function for the NACA 00xx profile family

Furthermore figure 1 is used to compare the computed results from XFOIL with the other data. The transition point in XFOIL was fixed to simulate a tripped boundary layer. Obviously XFOIL slightly underpredicts the drag coefficient, which is a known phenomenon [8]. XFOIL was developed in 1986 and uses for the boundary layer constants the values that were considered state of the art at that time. Meanwhile new experimental results [9] indicate that the constants in the b.l. equations should be adapted. As the gradient of the thickness function is more influenced by the potential flow around the foil and the b.l. constants would rather influence the overall level, a shift of the curve would only show up in the value of C_F in the following approximation of the XFOIL-results:

$$C_D = C_F \cdot \left[1 + 2.6045 \cdot \frac{t}{c} + 1.716 \cdot \left(\frac{t}{c} \right)^2 + 5.568 \cdot \left(\frac{t}{c} \right)^3 \right] \tag{4}$$

In figure 1 C_F is chosen so as to match the 12% data points. It is important to understand that the values of C_F in equations 3 and 4 are not identical. It can be seen, that Hoerner's equation and XFOIL only differ at low *t/c* ratios.

Figure 1 is only valid for the NACA 00xx family. A similar diagram could be drawn for other profile families. The constants in equations 2 and 3 would have to change and would be unique to each family.

2.2 The laminar skin friction coefficient of the flat plate

Since the first part of the flow is always laminar, we need the friction coefficient for laminar and turbulent flow to compute the total resistance of the mixed flow for the flat plate. For laminar flow the skin friction coefficient is well established and can be taken from any textbook:

$$C_{F,\,lam} = \frac{1.328}{\sqrt{Re_x}} \tag{5}$$

2.3 The turbulent skin friction coefficient of the flat plate

The integration of the local skin friction coefficient along the flat plate in 2-D flow from the leading edge to the location *x* yields the total friction coefficient C_F as a function of *x*. In an idealized condition, where the flow is turbulent right from the leading edge, one would call C_F the friction coefficient for fully turbulent flow. Since in the real world there will be always, even with a boundary layer trip, a very short laminar portion at the start of the b.l., $C_{F,\,turb}$ is a theoretically extrapolated value. As already indicated, new experimental results have been published in the last 15 years, which brought new insight into the problem through the application of the method of oil-film interferometry. This method allows the direct measurement of the local skin friction coefficient, independently of the measurement of the velocity profile close to the wall. These results have led to a reevaluation of the constants in the Coles-Fernholz equation. With each newly published PhD thesis the constants change a little bit, but these latest changes are insignificant for practical work. A good summary of the

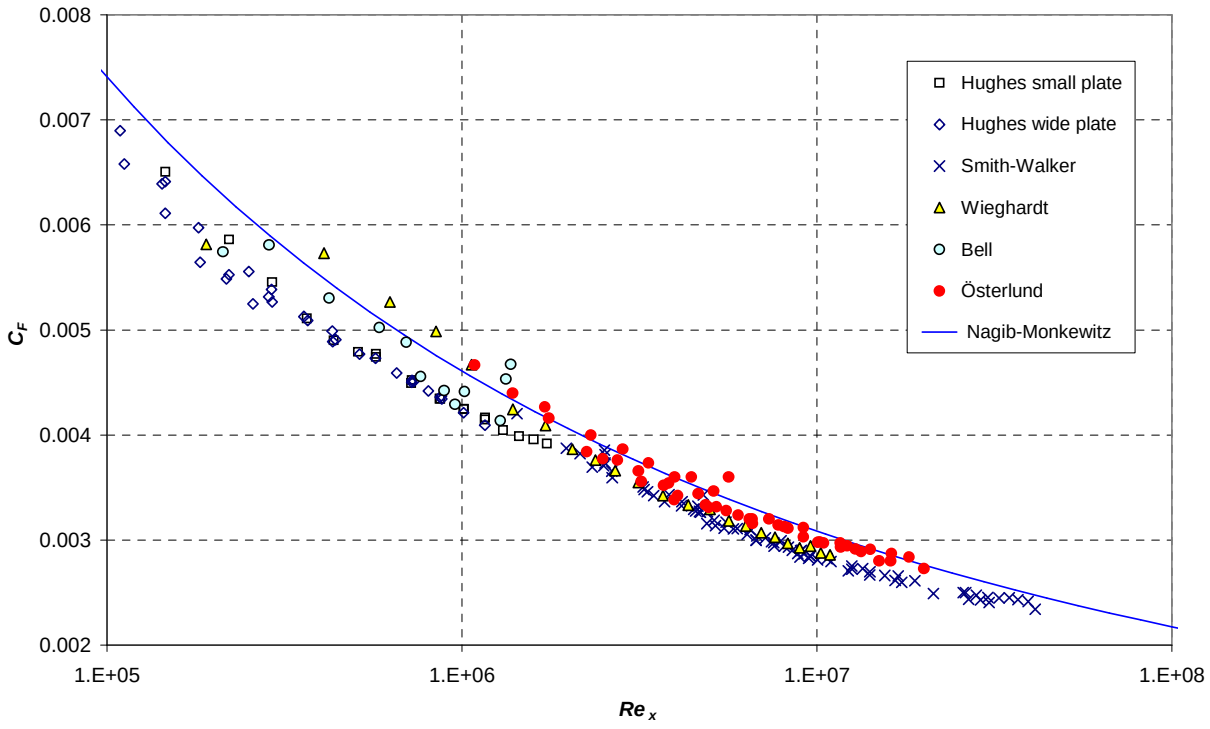

Figure 2. Total skin friction coefficient for the turbulent flow over a flat plate

current knowledge about turbulent, flat plate boundary layers is given by Nagib et al. [9]. The equations in [9] allow the calculation of the total skin friction coefficient as a function of the Reynolds number based on the length of the flat plate. The result is depicted in figure 2. The historical experimental data in figure 2 are taken from [10-12]. Hughes results are corrected for the edge effects according to [13]. Österlund [14] used the new oil-film interferometry; compared to his data the older measurements gave lower values for the total skin friction. This might be an explanation for the underprediction of the profile drag with b.l. programs that were "tuned" to the earlier test results. Experiments below a Reynolds number of 10^6 are sparse. Hughes plates seem to have had a laminar entrance that caused a reduction in the total skin friction coefficient. He used pins at the leading edge for turbulence stimulation. It seems difficult to achieve fully turbulent flow at the lower Reynolds numbers. Even without experimental proof it can be assumed, based on the theoretical background, that the fully turbulent flow is currently best described by the Nagib-Monkewitz approximation also below $Re = 10^6$. This approximation can be replaced by equation 5 within ± 0.01%.

$$C_{F,turb} = 0.549 \cdot \left[\log(Re_x) + 0.09\right]^{-2.6457} \tag{6}$$

2.4 The treatment of mixed flow for the flat plate

The flow is laminar up to the transition point and afterwards turbulent. In boundary layer codes there is a switch from the laminar to the turbulent equations at the transition point. Displacement, momentum and energy thickness of the laminar boundary layer at that point are taken as starting values for the turbulent computation. In reality the transition does not take place at once but happens within a transition zone. The length of this zone depends on the local Reynolds number and on the pressure gradient. A simple prediction formula for the total skin friction of the plate can only be a crude approximation of such a complex process, even if the transition point is known. Before the advent of computers Prandtl's method [15] was considered the best choice for the prediction of such flows. For a flat plate with the length l and the transition point at x_{tr} the skin friction is:

$$C_F = C_{F,turb}(l) + \left[C_{F,lam}(x_{tr}) - C_{F,turb}(x_{tr})\right] \cdot \frac{x_{tr}}{l} \tag{7}$$

i.e. in the fully turbulent total resistance the turbulent portion up to the transition point is replaced by the laminar resistance. When calculating these replacements, the Reynolds number in the equation for the friction coefficients must be based on the distance from the leading edge to the transition point.

3. THE DRAG COEFFICIENT AT ZERO LIFT FOR A TRIPPED BOUNDARY LAYER

If we follow Hoerner's proposal, equations 3-7 should be sufficient to predict the drag coefficient of a NACA 0012 profile. At this point we must discuss the mechanism of a boundary layer trip. A boundary layer will only become turbulent, if the Reynolds number based on the location of the trip is sufficiently high and if the roughness elements reach high enough into the b.l. Braslow et al. [16] recommend a grit of sparsely distributed carborundum particles where the particle height is equal to its width. Let k be the roughness height, then the roughness Reynolds number should be:

$$Re_k = \frac{u_k \cdot k}{\nu} = 600 \tag{8}$$

If Re_k is smaller, the b.l. will stay laminar, if Re_k is larger, there will be an additional drag, caused by the roughness. This mechanism works, if the trip location x_0 fulfills the following condition:

$$Re_0 = \frac{U_\infty \cdot x_0}{\nu} \geq 10^5 \tag{9}$$

Smaller Re_0 require a much higher roughness to trigger the transition, which will create an additional drag. These effects are illustrated in figure 3. The approximation by McCroskey for a trip at 5% chord is shown as a dashed black line. This is his best guess based on all available experimental data, but it is also interesting to look at the details of some of the test data. It is obviously difficult to trip the b.l. below the Reynolds number of 10^6. A 60-grit roughness, wrapped all around the leading edge, from 5% at the lower surface to 5% at the upper surface does not trip the b.l. at $Re_c = 7 \cdot 10^5$, because Re_0 is only $3.5 \cdot 10^4$. In Loftin's test the roughness is increased and extended to 8%. This increases the drag significantly but still does not avoid laminar flow at $Re_c = 7 \cdot 10^5$. Kerho and Bragg reported in [19] for $Re_c = 7.5 \cdot 10^5$ that a roughness height of 350µm at 5% chord resulted in a transition zone from 6% to 45% chord length. This indicates a very stable laminar b.l., even in the area of increasing pressure, because the NACA 0012 section has its minimal pressure at 12% chord.

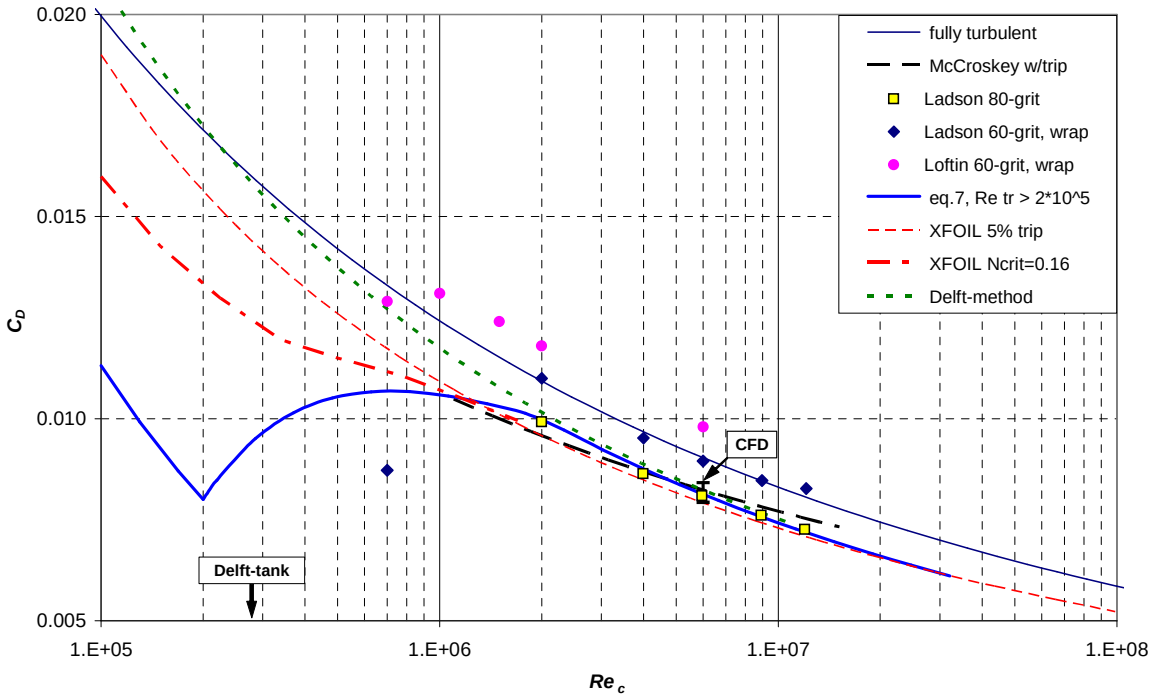

designation	aver. particle size	distribution	trip geometry	reference
Ladson 80-grit	185 µm	5-6%	strip	[17]
Ladson 60-grit, wrap	260 µm	± 5%	all around l.e.	[17]
Loftin 60-grit, wrap	280 µm	± 8%	all around l.e.	[18]

Figure 3. Profile drag at zero lift for the NACA 0012 wing section with b.l.-trip

If the b.l. can not be made turbulent below $Re_c = 10^6$, the question arises, if this kind of mixed flow can be predicted. The results of an XFOIL analysis are also depicted in Figure 3. If the transition point is fixed at 5%, XFOIL gives good results above $Re_c = 1.4 \cdot 10^6$. Below this value the computed drag is too high, because the transition does not take place at the tripping device, as predicted in equation 9. At the lower Reynolds numbers it is more realistic to use XFOIL with free transition. Ncrit was set to 0.16, because that gave a transition point at 5% chord for $Re_c = 1.4 \cdot 10^6$. It is also interesting to compare the XFOIL-results with CFD-results of RANS solvers [20]. The vertical bar in figure 3 indicates the variation of the results, caused by the choice of the turbulence model. Considering the relatively high Reynolds number and the fixed transition point which both simplify the solution, there is no advantage over XFOIL. This is also stated in [8].

At last equation 7 is used to predict the mixed flow. For the wing section the length l in equation 7 is replaced by the chord. The transition Reynolds number is calculated from:

$$Re_{tr} = Max\left\{2 \cdot Re_0,\, 2 \cdot 10^5\right\}$$
$$\text{and} \quad x_{tr} = \frac{Re_{tr}}{Re_c} \cdot c \tag{10}$$

In this formula Re_0 is multiplied by a factor 2, because there is a transition zone and the turbulent character will not develop immediately at the tripping device. The result is the blue line in figure 3. At the lower end, the curve merges with the line for fully laminar flow.

To summarize the findings one must conclude, that none of the curves matches the experimental data and the prediction of the drag is only possible above $Re_c = 10^6$. At lower Reynolds numbers the situation is uncertain because the dependence of the transition zone on roughness height, roughness position and Reynolds number is

unknown and can not be simulated in XFOIL either. Having this said, it is not possible to predict the drag of a model keel in the towing tank, if the model hull is less than 5 meters long. This can be shown, taking the experiments at the Delft University as an example. The experiments for the Delft Systematic Yacht Hull Series started 40 years ago and the database has been updated continuously to keep track with the development in modern yacht design. The details of the tripping devices are only described in the earlier papers [21]. At the lower end Froude number of 0.2 the Reynolds number based on average chord length of the keel is $2.7 \cdot 10^5$. This Reynolds number is marked in figure 3. From the grit information it follows that $Re_k = 813$ and $Re_0 = 8245$. This indicates that turbulent flow was most likely not achieved because Re_0 is an order of magnitude too small. In the Delft procedure the drag is measured twice with carborundum strips of different widths. The drag for zero width is calculated by extrapolation. This linear extrapolation must be called questionable, if the transition-status of the b.l. in the two tests is not known. The green dotted line represents the Delft method of combining equation 3 with the skin friction coefficient of the ITTC-57 line. This line is used at Delft for the scaling of the keel drag. Figure 3 shows that the usage of this line at model scale assumes fully turbulent flow. Whether the described extrapolation leads to the required drag value for fully turbulent flow is also questionable. Based on the above, all results for the keel drag derived from model tests at the Delft towing tank should be used with caution.

4. THE DRAG COEFFICIENT AT ZERO LIFT FOR FREE TRANSITION

Free transition is important for the prediction of the drag for the full size yacht. Typically a 10 meter yacht at a Froude number of 0.2 (4 knots) would have $Re_c = 3 \cdot 10^6$. The case for free transition is depicted in figure 4. McCroskey's best estimate is again shown by the dashed black line. The earliest experiments were conducted in 1939 in the Variable Density Tunnel [22], which has a high turbulence level. A much lower level was achieved in 1949 in the Langley Low-Turbulence Pressure Tunnel [18]. These results must be considered as the best ones available, because the later measurements by Ladson in the same tunnel [17] were subject to a higher and unknown (!) turbulence level. Ladson writes [p. 2] "This increase" (of the turbulence level) "was the result of successive damage to the heat exchanger because of freezing as well as deterioration of the screens". His drag data is on the level of the VDT of 1939. At Reynolds numbers below $5 \cdot 10^5$ the drag rises, because the fully laminar flow separates at the rear end of the foil. Only after the transition to turbulent flow the flow remains attached up to the trailing edge. Between $Re_c = 7.5 \cdot 10^5$ and $Re_c = 2.25 \cdot 10^6$ the transition point moves from a point at 65% chord to 44% [19]. This decrease of the laminar portion and therefore increase of the drag counterbalances the decrease of the turbulent skin friction coefficient with increasing Reynolds number. The overall drag coefficient of the foil is therefore almost constant between $Re_c = 10^6$ and $Re_c = 10^7$. The prediction of this behavior is difficult. The Delft-method is about as wrong as the assumption of fully turbulent flow.

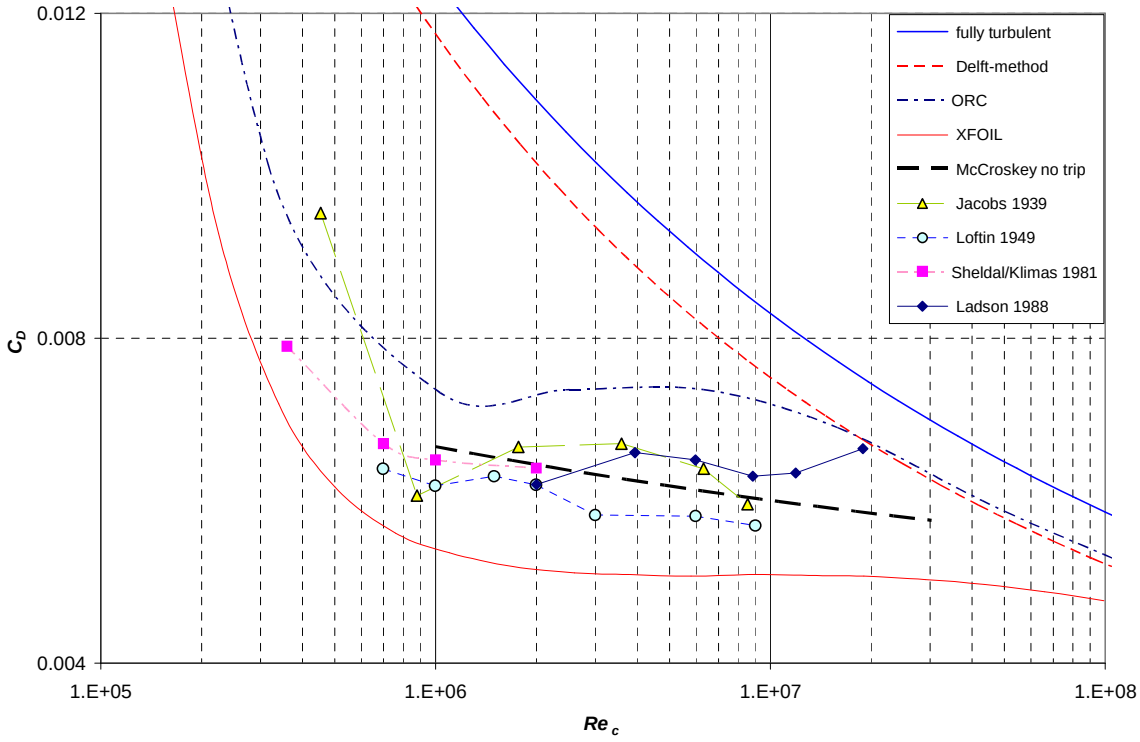

Figure 4. Profile drag at zero lift for the NACA 0012 wing section with free transition

The XFOIL-predictions (Ncrit = 9) are about 14-20% too low. ORC uses tabulated values for the drag coefficient [1]; the curve in figure 4 is a spline interpolation of these values. The curve is about 26% too high. Why the ORC choose such high values is not known. The best solution for a VPP seems to be the spline interpolation of tabulated values. A different set of points is required for each wing section and thickness ratio.

5. CONCLUSION

5.1 Tank testing

For large models (> 5m) the drag of the keel can be predicted from equation 7, if a suitable b.l. trip is used. In this case the hull drag can be determined by subtracting the predicted keel drag and an estimated interference drag from the measured total drag of the model. If the model is tested with a drift angle, the drag increase for the keel can be taken from [2] or computed with XFOIL. For small models the test with a keel is not meaningful, because the forces can not be predicted reliably. If the keel is needed, because the flow around the hull is altered by the keel at larger heel and drift angles, then the keel forces need to be measured separately with the help of a load cell dynamometer between keel and hull.

5.2 Full size prediction

For the drag of the keel at full size in the heeled attitude with a drift angle, there is no correlation line that could be used. One can only recommend, using the measured drag polars in [2] at a Reynolds number close to the speed range of interest. The dependence on the Reynolds number could be neglected between $Re_c = 10^6$ and $Re_c = 10^7$. If higher accuracy is needed, the polar curve could be shifted parallel to McCroskeys line. A further possibility would be the use of XFOIL and change Ncrit iteratively until the results match the polars in [2]. In this case XFOIL could be regarded as an interpolation tool for the experimental results. In summary, there is no simple method to calculate the keel drag in a VPP.

6. REFERENCES

1. Offshore Racing Congress, VPP Documentation 2012. [Online]. Available: http://www.orc.org/rules/
2. Abbott, I.H., v. Doenhoff, A.E., *Theory of Wing Sections*, New York, USA: Dover, 1959
3. Drela, M., Youngren, H., XFOIL Computer Program. [Online]. Available: http://web.mit.edu/drela/Public/web/xfoil/
4. Squire, H.B., Young, B.A., "The Calculation of the Profile Drag of Aerofoils", ARC, R&M No. 1838, 1937
5. Helmbold, H.B., "Zur Berechnung des Profilwiderstands", *Ingenieur-Archiv*, Band 17, pp.273-279, 1949
6. Hoerner, S.F., *Fluid-Dynamic Drag*, Midland Park, NJ: published by the author, 1965
7. McCroskey, W.J., "A critical assessment of wind tunnel results for the NACA 0012 airfoil", NASA TM 100019, 1987
8. Maughmer, M.D., Coder, J.G., (2010), "Comparison of Theoretical Methods for Predicting Airfoil Aerodynamic Characteristics", The Pennsylvania State University, USA. [Online]. Available: http//handle.dtic.mil/100.2/ADA532502
9. Nagib, H.M., Chauhan, K.A., Monkewitz, P.A., "Approach to an asymptotic state for zero pressure gradient turbulent boundary layers", *Phil. Trans. R. Soc. A* **365**, pp 755-770, 2007
10. Hughes, G., “Frictional resistance of smooth plane surfaces in turbulent flow”, *Trans. I.N.A.*, Vol. 94, pp. 287-322, 1952
11. Smith, D.W., Walker, J.H., "Skin-friction measurements in incompressible flow", NACA TN 4231, 1958
12. Coles, D., "The young person's guide to the data", in *Proc. Computation of turbulent boundary layers-1968 AFOSR-IFP-Stanford Conf.*, Vol. 2, pp 1-46
13. Davies, E.B., Young, A.D., "Streamwise Edge Effects in the Turbulent Boundary Layer on a Flat Plate of Finite Aspect Ratio”, ARC, R&M No. 3367, 1963
14. Österlund, J.M., “Experimental studies of zero pressure-gradient turbulent boundary layer flow”, Ph.D. diss., Dept. Mechanics, KTH Stockholm, Sweden, 1999

15. Prandtl, L., Betz, A., "Über den Reibungswiderstand strömender Luft", in *Ergebnisse der Aerodynamischen Versuchsanstalt zu Göttingen, III. Lieferung"*, München, Germany: Oldenburg Verl., 1935, pp 4-5
16. Braslow, A.L., Hicks, R.M., Harris, R.V., "Use of grit-type boundary-layer-transition trips on wind-tunnel models", NASA TN D-3579, 1966
17. Ladson, C.L., "Effects of Independent Variation of Mach and Reynolds Numbers on the Low-Speed Aerodynamic Characteristics of the NACA 0012 Airfoil Section", NASA TM 4074, 1988
18. Loftin, L.K., Smith, H.A., "Aerodynamic characteristics of 15 NACA airfoil sections at seven Reynolds numbers", NACA TN 1945, 1949
19. Kerho, M.F., Bragg, M.B., "Airfoil Boundary-Layer Development and Transition with Large Leading-Edge Roughness", *AIAA Journal*, Vol. 35, No. 1, 1997
20. Freeman, J.A., Roy, C.J., "Verification and Validation of RANS Turbulence Models in Commercial Flow Solvers", *50th AIAA Aerospace Sciences Meeting*, Nashville, TN, 2012
21. Gerritsma, J., Onnink, R., Versluis, A., "Geometry, resistance and stability of the Delft Systematic Yacht Hull Series", in *Proc. 7nth HISWA Symp.*, Amsterdam, NL, 1981
22. Jacobs, E.N., Abbott, I.H., "Airfoil Section Data Obtained in the NACA VDT as Affected by Support Interference and Other Corrections", NACA Rep. No. 669, 1939